Chapter 5

A high-order fully discrete method for non-linear time-fractional reaction-diffusion equation with non-smooth solutions

This chapter is dedicated to the formulation of a high-order approximation technique for solving the following non-linear time-fractional reaction-diffusion equation (TFRDE)

$$ {}_0^C D_t^\alpha u(x,t) - p(t)\frac{\partial^2 u(x,t)}{\partial x^2} + q(t)u(x,t) + G(u(x,t)) = f(x,t),\ (x,t) \in (a,b)\times(0,T], \tag{5.1}$$

with initial and boundary conditions

$$\begin{cases} u(x,0) = \phi(x), & x \in [a,b], \\ u(a,t) = \psi_1(t), & t \in (0,T], \\ u(b,t) = \psi_2(t), & t \in (0,T], \end{cases} \tag{5.2}$$

where ${}_0^C D_t^\alpha$ denotes the Caputo differential operator of fractional order $\alpha \in (0,1)$ defined in equation (1.14). Here, the coefficients satisfy $0 < c_1 \le p(t)$ and $0 < c_2 \le q(t)$, along with the non-linear term $G(u)$ for which $G'(u) > 0$ holds. Furthermore, it can be noted that f, ϕ, ψ_1, and ψ_2 are sufficiently smooth within their specified domains. Throughout this work, we make the assumption of $G(0) = 0$ without any loss of generality.

The presence of a singularity near the initial time $t = 0$ is a well-recognized characteristic of solutions to equations (5.1)-(5.2). Furthermore, it should be noted that the derivatives of the solution satisfy the prescribed regularity requirements, as outlined in [103]

$$\left|\frac{\partial^l u}{\partial x^l}\right| \leq c, \text{ for } 0 \leq l \leq 8, \tag{5.3}$$

$$\left|\frac{\partial^l u}{\partial t^l}\right| \leq c(1 + t^{\alpha - l}), \text{ for } 0 \leq l \leq 3, \tag{5.4}$$

where the constant c is to be regarded as positive, and does not vary with respect to either time t or spatial x variables. Equation (5.4) highlights the fact that $u(x,t)$ demonstrates a weak singularity at $t = 0$, causing the unbounded behavior of the time derivative $|\partial u/\partial t|$ as $t \to 0^+$. Dealing with a weak initial singularity presents considerable challenges, encompassing both practical and theoretical aspects, when employing traditional numerical techniques. This challenge arises from their limited ability to precisely examine how the solution behaves in the neighborhood of singular points. Consequently, the design of efficient numerical methods capable of addressing the singularity at $t = 0$ with efficacy becomes a challenging and demanding task.

The central objective of this chapter is to devise and analyze a high-order numerical method designed to address the variable coefficient non-linear TFRDE (5.1)-(5.2) with non-smooth data. The proposed technique hinges on Alikhanov's L2-1_σ approximation for the Caputo fractional derivative, skillfully implemented on a graded mesh along with the adoption of a highly accurate non-polynomial parametric quintic spline scheme to manage the spatial derivatives. The utilization of the graded mesh allows us to effectively handle the initial layer in the solution, achieved through the use of an exceptionally fine mesh near $t = 0$. The analysis of stability and convergence for the developed numerical method is conducted thoroughly using the discrete energy method. The convergence analysis reveals that the developed numerical method attains an order of $\mathcal{O}(N_t^{-\min\{\theta\alpha,2\}}, h^{4.5})$, where h corresponds to the spatial step size, N_t represents the total number of time grid points, and θ is the grading parameter.

The organization of the chapter is outlined as follows: Section 5.1 initiates with the development of a high-order numerical method for variable coefficient non-linear TFRDE. In the subsequent section, Section 5.2, our focus shifts towards the examination of the method's unique solvability, stability, and convergence properties. To evaluate its performance, Section 5.3 presents a comprehensive set of numerical results, underscoring the efficiency and accuracy of the proposed approach. Finally, Section 5.4 serves as the concluding segment of this chapter, offering a concise summary of the key findings and contributions.

5.1 A high-order fully discrete numerical scheme

5.1.1 High-order discretization of time-fractional derivative

Suppose N_t is a positive integer. To partition the interval $[0, T]$, we utilize a graded mesh, where the mesh points are represented as $t_j = T\left(\frac{j}{N_t}\right)^\theta$ for $0 \le j \le N_t$. Users can select the grading parameter θ according to their preferences, provided that θ meets the condition $\theta \ge 1$.

Additionally, define $\Delta t_j = t_j - t_{j-1}$ for $1 \le j \le N_t$, and introduce the relation $t_{j+\sigma} = t_j + \sigma\Delta t_{j+1}$ for $0 \le j \le N_t - 1$. Using Alikhanov's formula (L2-1_σ), we compute an approximation for the Caputo derivative of the function v, where v belongs to the space $C[0,T]\cap C^3(0,T]$, at the time level $t_{j+\sigma}$ given in [18]

$$ {}_0^C D_t^\alpha v(t_{j+\sigma}) = w_{j,j}^{(\alpha,\sigma)} v(t_{j+1}) - \sum_{i=1}^{j}\left(w_{j,i}^{(\alpha,\sigma)} - w_{j,i-1}^{(\alpha,\sigma)}\right) v(t_i) - w_{j,0}^{(\alpha,\sigma)} v(t_0) + \mathcal{R}_t^{j+\sigma}. \tag{5.5}$$

Here, the term $\mathcal{R}_t^{j+\sigma}$ representing the local truncation error, which is bounded by the following lemma.

Lemma 5.1. *[18] Suppose that the function $v \in C[0,T]\cap C^3(0,T]$, meets the assumptions provided in (5.4). Then the local truncation error $\mathcal{R}_t^{j+\sigma}$, of the approximation (5.5) satisfies the following bound:*

$$\left|\mathcal{R}_t^{j+\sigma}\right| \le c\, t_{j+\sigma}^{-\alpha} N_t^{-\min\{\theta\alpha, 3-\alpha\}},\ 0 \le j \le N_t - 1,$$

where $0 \le \sigma \le 1$.

By removing the term $\mathcal{R}_t^{j+\sigma}$ from equation (5.5), we get the following difference operator

$$\Delta_t^\alpha v(t_{j+\sigma}) = w_{j,j}^{(\alpha,\sigma)} v(t_{j+1}) - \sum_{i=1}^{j}\left(w_{j,i}^{(\alpha,\sigma)} - w_{j,i-1}^{(\alpha,\sigma)}\right) v(t_i) - w_{j,0}^{(\alpha,\sigma)} v(t_0). \tag{5.6}$$

The values of the coefficients $w^{(\alpha,\sigma)}$'s are provided as follows: $w_{0,0}^{(\alpha,\sigma)} = \Delta t_1^{-1} r_{0,0}^{(\alpha,\sigma)}$, and for $j \ge 1$

$$w_{j,i}^{(\alpha,\sigma)} = \begin{cases} \Delta t_{i+1}^{-1}\left(r_{j,0}^{(\alpha,\sigma)} + s_{j,0}^{(\alpha,\sigma)}\right), & i = 0, \\ \Delta t_{i+1}^{-1}\left(r_{j,i}^{(\alpha,\sigma)} + s_{j,i-1}^{(\alpha,\sigma)} - s_{j,i}^{(\alpha,\sigma)}\right), & 1 \le i \le j-1, \\ \Delta t_{i+1}^{-1}\left(r_{j,j}^{(\alpha,\sigma)} + s_{j,j-1}^{(\alpha,\sigma)}\right), & i = j, \end{cases} \tag{5.7}$$

with

$$r_{j,j}^{(\alpha,\sigma)} = \frac{\sigma^{1-\alpha}}{\Gamma(2-\alpha)}\Delta t_{j+1}^{1-\alpha}, \text{ for } j \geq 0, \tag{5.8}$$

and for $j \geq 1$, $0 \leq i \leq j-1$

$$r_{j,i}^{(\alpha,\sigma)} = \frac{1}{\Gamma(1-\alpha)}\int_{t_i}^{t_{i+1}} (t_{j+\sigma} - s)^{-\alpha} ds, \tag{5.9}$$

$$s_{j,i}^{(\alpha,\sigma)} = \frac{1}{\Gamma(1-\alpha)}\frac{2}{(t_{i+2}-t_i)}\int_{t_i}^{t_{i+1}} (t_{j+\sigma} - s)^{-\alpha}(s - t_{i+1/2}) ds. \tag{5.10}$$

Lemma 5.2. [18] *Assume that $1 \geq \sigma \geq 1-\alpha/2$, and for $1 \leq j \leq N_t - 1$, the local mesh ratio ν_j, defined as $\nu_j = \frac{\Delta t_{j+1}}{\Delta t_j}$, falls within the range of $62 \geq \nu_j \leq 3/4$. Then*

(i). $w_{j,0}^{(\alpha,\sigma)} > \dfrac{t_{j+\sigma}^{-\alpha}}{\Gamma(1-\alpha)} > 0, \ j \geq 0.$

(ii). $(2\sigma-1)w_{1,1}^{(\alpha,\sigma)} - \sigma w_{1,0}^{(\alpha,\sigma)} > 0.$

(iii). $w_{j,1}^{(\alpha,\sigma)} > w_{j,0}^{(\alpha,\sigma)}, \quad j \geq 1.$

(iv). *If* $\nu_{i-1}^2(\nu_{i-1}+1) \geq \dfrac{\nu_i}{\nu_i+1}$ *for* $2 \leq i \leq j,$ *with* $j \geq 2,$ *then* $w_{j,i-1}^{(\alpha,\sigma)} < w_{j,i}^{(\alpha,\sigma)}.$

(v). *If* $\nu_{j-1}^2\left(2 - \dfrac{1}{\sigma} + \nu_j(\nu_j+2)\right) \geq \dfrac{\nu_j(\nu_j+1)}{\nu_{j-1}+1}$ *for* $2 \leq j \leq N_t,$ *then*

$$(2\sigma-1)w_{j,j}^{(\alpha,\sigma)} - \sigma w_{j,j-1}^{(\alpha,\sigma)} > 0.$$

Equation (5.1) assumes the following form at $t = t_{j+\sigma}$

$$ {}_0^C D_t^{\alpha} u^{j+\sigma}(x) - p^{j+\sigma}\frac{\partial^2 u^{j+\sigma}(x)}{\partial x^2} + q^{j+\sigma}u^{j+\sigma}(x) + G(u^{j+\sigma}(x)) = f^{j+\sigma}(x),$$

$$x \in (a,b), \ 0 \leq j \leq N_t - 1, \tag{5.11}$$

with initial and boundary conditions

$$\begin{cases} u(x,0) = \phi(x), & x \in [a,b], \\ u^j(a) = \psi_1(t_j), & 1 \le j \le N_t, \\ u^j(b) = \psi_2(t_j), & 1 \le j \le N_t, \end{cases} \tag{5.12}$$

where we denote $u^{j+\sigma}(x) = u(x, t_{j+\sigma})$, $p^{j+\sigma} = p(t_{j+\sigma})$, $q^{j+\sigma} = q(t_{j+\sigma})$, and $f^{j+\sigma}(x) = f(x, t_{j+\sigma})$.

Incorporating the L2-1_σ approximation, which is applied on a non-uniform graded mesh in accordance with equation (5.5), into equation (5.11), results in the following semi-discrete scheme

$$w_{j,j}^{(\alpha,\sigma)} u^{j+1}(x) - \sum_{i=1}^{j} \left(w_{j,i}^{(\alpha,\sigma)} - w_{j,i-1}^{(\alpha,\sigma)} \right) u^i(x) - w_{j,0}^{(\alpha,\sigma)} u^0(x) - p^{j+\sigma} \frac{\partial^2 u^{j+\sigma}(x)}{\partial x^2} + q^{j+\sigma}$$
$$\times\, u^{j+\sigma}(x) + G(u^{j+\sigma}(x)) = f^{j+\sigma}(x) + \mathcal{R}_t^{j+\sigma},\ x \in (a,b),\ 0 \le j \le N_t - 1.$$

Further

$$w_{j,j}^{(\alpha,\sigma)} u^{j+1}(x) - \sum_{i=1}^{j} \left(w_{j,i}^{(\alpha,\sigma)} - w_{j,i-1}^{(\alpha,\sigma)} \right) u^i(x) - w_{j,0}^{(\alpha,\sigma)} u^0(x) - p^{j+\sigma} \frac{\partial^2 u^{j,\sigma}(x)}{\partial x^2} + q^{j+\sigma} u^{j,\sigma}(x)$$
$$+\, G(u^{j,\sigma}(x)) = f^{j+\sigma}(x) + \mathcal{R}_t^{j+\sigma} + (\mathcal{R}_t^{\alpha})^{j,\sigma},\ x \in (a,b),\ 0 \le j \le N_t - 1, \tag{5.13}$$

where $u^{j,\sigma} = \sigma u^{j+1} + (1-\sigma) u^j$ and a bound for $(\mathcal{R}_t^{\alpha})^{j,\sigma}$ can be obtained by invoking the following Lemma 5.3.

Lemma 5.3. *[18] Let's assume that $v(t) \in C^2(0,T]$. Then*

$$\left| v(t_{j+\sigma}) - \{\sigma v(t_{j+1}) + (1-\sigma) v(t_j)\} \right| \le \frac{\Delta t_{j+1}^2}{8} \max_{\tau \in (t_j, t_{j+1})} |v''(\tau)|,\ \textit{for } 1 \le j \le N_t - 1.$$

5.1.2 High-order non-polynomial spline scheme

This subsection is dedicated to provide a spatial discretization scheme of significantly higher order designed for addressing the equations (5.1)-(5.2). To achieve this, we define a positive integer N_x and proceed to partition the interval $[a, b]$ into N_x subintervals, characterized by the notation $\Omega_x : a = x_0 < x_1 < \cdots < x_{N_x} = b$. Consider $x_m = a + mh$, where the mesh width is defined as $h = \frac{b-a}{N_x}$. Let's denote the exact solution of the problem (5.1)–(5.2) as $u(x,t)$. Simplifying our representation, we adopt the notations $u_m^j = u(x_m, t_j)$ and $f_m^j = f(x_m, t_j)$, for $0 \le m \le N_x$ and $0 \le j \le N_t$. Furthermore, we will use the notation U_m^j to represent the approximation of u_m^j. Now, we define two sets: $\mathcal{D}_h = \{\vartheta | (\vartheta_0, \vartheta_1, \cdots, \vartheta_{N_x})\}$, and $\mathcal{D}_h^* = \{\vartheta | (\vartheta_0, \vartheta_1, \cdots, \vartheta_{N_x}), \vartheta_0 = \vartheta_{N_x} = 0\}$. Thus, for any grid function $\vartheta \in \mathcal{D}_h$, we will represent

$$\begin{aligned}
\delta_x \vartheta_{m+\frac{1}{2}} &= \frac{1}{h}(\vartheta_{m+1} - \vartheta_m), \quad \delta_x^2 \vartheta_m = \frac{1}{h}\left(\delta_x \vartheta_{m+\frac{1}{2}} - \delta_x \vartheta_{m-\frac{1}{2}}\right), \\
\delta_x^3 \vartheta_{m+\frac{1}{2}} &= \frac{1}{h}(\delta_x^2 \vartheta_{m+1} - \delta_x^2 \vartheta_m), \quad \delta_x^4 \vartheta_m = \frac{1}{h}\left(\delta_x^3 \vartheta_{m+\frac{1}{2}} - \delta_x^3 \vartheta_{m-\frac{1}{2}}\right).
\end{aligned}$$

Now, we provide $\mathcal{H}_q$: a high-order parametric quintic spline operator that plays a crucial role in achieving a high-order spatial discretized scheme for (5.1)–(5.2).

Definition 5.1. [50, 51, 100] For a given mesh Ω_x, a function $\mathcal{P}_{\Omega_x}(x;\varsigma)$ belonging to $C^4[a, b]$ is termed a parametric quintic spline with parameter $\varsigma > 0$, if its restriction $\mathcal{P}_{\Omega_x,m}(x;\varsigma) = \{\mathcal{P}_{\Omega_x}(x;\varsigma)\}_{[x_{m-1},x_m]}$, where $1 \le m \le N_x$, satisfy the condition $\mathcal{P}_{\Omega_x,m}(x_j) = \vartheta_j$ for $j = m-1, m$ and

$$\mathcal{P}^{(4)}_{\Omega_x,m}(x) + \varsigma^2 \mathcal{P}''_{\Omega_x,m}(x) = (\mathcal{F}_m + \varsigma^2 \tilde{\omega}_m)\frac{(x - x_{m-1})}{h} + (\mathcal{F}_{m-1} + \varsigma^2 \tilde{\omega}_{m-1})\frac{(x_m - x)}{h}, \tag{5.14}$$

where $\mathcal{P}''_{\Omega_x,m}(x_j) = \tilde{\omega}_j$ and $\mathcal{P}^{(4)}_{\Omega_x,m}(x_j) = \mathcal{F}_j$, $j = m-1, m$.

By solving equation (5.14) for $\mathcal{P}_{\Omega_x,m}$, we obtain

$$\mathcal{P}_{\Omega_x,m}(x) = \rho\vartheta_m + \bar{\rho}\vartheta_{m-1} + \frac{h^2}{6}\left(\chi_1(\rho)\tilde{\omega}_m + \chi_1(\bar{\rho})\tilde{\omega}_{m-1}\right) + \left(\frac{h}{\tilde{\gamma}}\right)^4 \left(\frac{\tilde{\gamma}^2}{6}\chi_1(\rho) - \chi_2(\rho)\right) \times \mathcal{F}_m + \left(\frac{h}{\tilde{\gamma}}\right)^4 \left(\frac{\tilde{\gamma}^2}{6}\chi_1(\bar{\rho}) - \chi_2(\bar{\rho})\right)\mathcal{F}_{m-1}, \tag{5.15}$$

where $\tilde{\gamma} = \varsigma h$, $\rho = \frac{(x-x_{m-1})}{h}$, $\bar{\rho} = 1-\rho$, $\chi_1(\rho) = \rho^3 - \rho$, and $\chi_2(\rho) = \rho - \frac{\sin\tilde{\gamma}\rho}{\sin\tilde{\gamma}}$.

Employing the constraints on the first and third derivatives' continuity of $\mathcal{P}_{\Omega_x}(x)$ at $x = x_m$, viz $\mathcal{P}'_{\Omega_x,m}(x_m) = \mathcal{P}'_{\Omega_x,m+1}(x_m)$ and $\mathcal{P}'''_{\Omega_x,m}(x_m) = \mathcal{P}'''_{\Omega_x,m+1}(x_m)$, we establish two relationships involving ϑ_j, $\tilde{\omega}_j$ and $\mathcal{F}_j$, $j = m-1, m, m+1$. Upon eliminating $\mathcal{F}_j$, we arrive at

$$\widetilde{p}\tilde{\omega}_{m-2} + \widetilde{q}\tilde{\omega}_{m-1} + \widetilde{s}\tilde{\omega}_m + \widetilde{q}\tilde{\omega}_{m+1} + \widetilde{p}\tilde{\omega}_{m+2} = (\delta_x^2 + \mu h^2\delta_x^4)\vartheta_m, \quad 2 \le m \le N_x - 2, \tag{5.16}$$

where $\mu = \frac{1}{\tilde{\gamma}^2}\left(\frac{\tilde{\gamma}}{\sin\tilde{\gamma}} - 1\right)$ and $\widetilde{p}$, $\widetilde{q}$, and $\widetilde{s}$ satisfying the equation $2\widetilde{p} + 2\widetilde{q} + \widetilde{s} = 1$.

The consideration of μ within the interval $\left(0, \frac{1}{2}\right)$ is dictated by the consistency relation outlined in [50]. However, it's noteworthy that utilizing μ values in this range yields an array of schemes with varying degrees of accuracy.

In addition to equation (5.16), we necessitate two additional equations, derivable from the subsequent formulation

$$-\mathcal{R}_m = \frac{d_{m-1}\vartheta_{m-1} + d_m\vartheta_m + d_{m+1}\vartheta_{m+1}}{h^2} + d^*_{m-1}\tilde{\omega}_{m-1} + d^*_m\tilde{\omega}_m + d^*_{m+1}\tilde{\omega}_{m+1}, \quad m = 1, N_x - 1.$$

Here, $\mathcal{R}_m$ denotes the local truncation error at $x = x_m$. Coefficients d's and d^*'s are unknown and must be determined such that $\mathcal{R}_m = \mathcal{O}(h^4)$ holds true for $m = 1, N_x - 1$.

In the preceding pair of equations, upon performing Taylor expansions at $x = x_m$, and considering $\mathcal{R}_m = \mathcal{O}(h^4)$ for $m = 1, N_x - 1$, we obtain

$$\left(d_{m-1}, d_m, d_{m+1}, d^*_{m-1}, d^*_m, d^*_{m+1}\right) = \left(-1, 2, -1, \frac{1}{12}, \frac{10}{12}, \frac{1}{12}\right) \quad m = 1, N_x - 1.$$

Subsequently, by eliminating the term representing local truncation error $\mathcal{R}_m$, we arrive at two equations as follows

$$\left(I + \frac{h^2}{12}\delta_x^2\right)\tilde{\omega}_m = \delta_x^2 \vartheta_m, \quad m = 1, N_x - 1. \tag{5.17}$$

By combining equations (5.16) and (5.17), we introduce the parametric quintic spline operator $\mathcal{H}_q$ as follows

$$\mathcal{H}_q \vartheta_m = \begin{cases} \left(I + \frac{h^2}{12}\delta_x^2\right)\vartheta_m, & m = 1, N_x - 1, \\ \widetilde{p}\vartheta_{m-2} + \widetilde{q}\vartheta_{m-1} + \widetilde{s}\vartheta_m + \widetilde{q}\vartheta_{m+1} + \widetilde{p}\vartheta_{m+2}, & 2 \le m \le N_x - 2. \end{cases} \tag{5.18}$$

Furthermore, for $\mu \in \left(0, \frac{1}{2}\right)$, we introduce the notation

$$\tilde{\delta}_x^2 \vartheta_m = \begin{cases} \delta_x^2 \vartheta_m, & m = 1, N_x - 1, \\ \left(\delta_x^2 + \mu h^2 \delta_x^4\right)\vartheta_m, & 2 \le m \le N_x - 2. \end{cases} \tag{5.19}$$

We proceed to employ Taylor expansions at $x = x_m$, leading us to the following result.

Lemma 5.4. *Suppose $\vartheta \in C^8[a, b]$. If*

$$\widetilde{p} = \frac{\mu}{12} - \frac{1}{240}, \quad \widetilde{q} = \frac{8\mu}{12} + \frac{1}{10}, \quad \widetilde{s} = -\frac{3\mu}{2} + \frac{97}{120}, \tag{5.20}$$

then the following result holds

$$\mathcal{R}_x = \mathcal{H}_q \frac{\partial^2 \vartheta}{\partial x^2}\bigg|_{x_m} - \tilde{\delta}_x^2 \vartheta_m = \begin{cases} -\frac{h^4}{240}\frac{\partial^6 \vartheta}{\partial x^6}\bigg|_{x_i} + \mathcal{O}(h^6), & m = 1, N_x - 1, \\ \mathcal{Q} h^6 \frac{\partial^8 \vartheta}{\partial x^8}\bigg|_{x_m} + \mathcal{O}(h^8), & 2 \leq m \leq N_x - 2, \end{cases} \tag{5.21}$$

where $\mathcal{Q} = -\frac{8\tilde{p}}{45} - \frac{\tilde{q}}{360} + \frac{126\mu}{10080} + \frac{1}{20160}$ *and* $\mu \in \left(0, \frac{1}{2}\right)$.

Remark 5.1. In the subsequent sections of this chapter, we adopt the values of $\tilde{p}$, $\tilde{q}$, and $\tilde{s}$, as specified in equation (5.20).

We will now analyze problem (5.13) while considering x at x_m for $1 \leq m \leq N_x - 1$. We have

$$w_{j,j}^{(\alpha,\sigma)} u_m^{j+1} - \sum_{i=1}^{j} \left(w_{j,i}^{(\alpha,\sigma)} - w_{j,i-1}^{(\alpha,\sigma)} \right) u_m^i - w_{j,0}^{(\alpha,\sigma)} u_m^0 - p^{j+\sigma} \left(u_{xx}\right)_m^{j,\sigma} + q^{j+\sigma} u_m^{j,\sigma}$$
$$+ G(u_m^{j,\sigma}) = f_m^{j+\sigma} + \mathcal{R}_t^{j+\sigma} + (\mathcal{R}_t^{\alpha})^{j,\sigma}, \quad 1 \leq m \leq N_x - 1, \; 0 \leq j \leq N_t - 1. \tag{5.22}$$

with initial and boundary conditions

$$\begin{cases} u_m^0 = \phi(x_m), & 0 \leq m \leq N_x, \\ u_0^j = \psi_1(t_j), & 1 \leq j \leq N_t, \\ u_{N_x}^j = \psi_2(t_j), & 1 \leq j \leq N_t. \end{cases} \tag{5.23}$$

Now, the application of the parametric quintic spline operator $\mathcal{H}_q$, established in equation (5.18), to both sides of the preceding equation (5.22) leads to

$$w_{j,j}^{(\alpha,\sigma)} \mathcal{H}_q u_m^{j+1} - \sum_{i=1}^{j} \left(w_{j,i}^{(\alpha,\sigma)} - w_{j,i-1}^{(\alpha,\sigma)} \right) \mathcal{H}_q u_m^i - w_{j,0}^{(\alpha,\sigma)} \mathcal{H}_q u_m^0 - p^{j+\sigma} \tilde{\delta}_x^2 u_m^{j,\sigma} + q^{j+\sigma}$$
$$\times \mathcal{H}_q u_m^{j,\sigma} + \mathcal{H}_q G(u_m^{j,\sigma}) = \mathcal{H}_q f_m^{j+\sigma} + \mathcal{R}_f, \quad 1 \leq m \leq N_x - 1, \; 0 \leq j \leq N_t - 1, \tag{5.24}$$

where $\mathcal{R}_f = \mathcal{R}_t^{j+\sigma} + (\mathcal{R}_t^{\alpha})^{j,\sigma} + \mathcal{R}_x$ and a bound for $\mathcal{R}_x$ can be obtained by invoking the Lemma 5.4. Now, by removing the error term $\mathcal{R}_f$, we get the subsequent fully discrete numerical scheme

$$\begin{aligned} w_{j,j}^{(\alpha,\sigma)}\mathcal{H}_q U_m^{j+1} - \sum_{i=1}^{j}\left(w_{j,i}^{(\alpha,\sigma)} - w_{j,i-1}^{(\alpha,\sigma)}\right)\mathcal{H}_q U_m^i - w_{j,0}^{(\alpha,\sigma)}\mathcal{H}_q U_m^0 - p^{j+\sigma}\tilde{\delta}_x^2 U_m^{j,\sigma} + q^{j+\sigma} \\ \times \mathcal{H}_q U_m^{j,\sigma} + \mathcal{H}_q G(U_m^{j,\sigma}) = \mathcal{H}_q f_m^{j+\sigma}, \quad 1 \le m \le N_x - 1, \ 0 \le j \le N_t - 1. \end{aligned} \tag{5.25}$$

Now, the matrix representation of equation (5.25) is given by

$$\begin{aligned} \mathcal{A}^j U^{j+1} + \sigma \mathcal{B} G(U^{j+1}) =& w_{j,0}^{(\alpha,\sigma)}\mathcal{B}U^0 + \sum_{i=1}^{j}\left(w_{j,i}^{(\alpha,\sigma)} - w_{j,i-1}^{(\alpha,\sigma)}\right)\mathcal{B}U^i + \mathcal{D}^j U^j - (1-\sigma) \\ & \times \mathcal{B}G(U^j) + \mathcal{B}f^{j+\sigma} + \mathcal{E}^j, \quad 0 \le j \le N_t - 1, \end{aligned} \tag{5.26}$$

where

$$\begin{aligned} &\mathcal{A}^j = \left[\left(w_{j,j}^{(\alpha,\sigma)} + \sigma q^{j+\sigma}\right)\mathcal{B} - \frac{\sigma p^{j+\sigma}}{h_x^2}\mathcal{K}\right], \quad \mathcal{D}^j = \left[\frac{(1-\sigma)p^{j+\sigma}}{h_x^2}\mathcal{K} - (1-\sigma)q^{j+\sigma}\mathcal{B}\right], \\ &U^{j+1} = \left[U_1^{j+1}, U_2^{j+1}, \ldots, U_{N_x-1}^{j+1}\right]^T, \quad G(U^{j+1}) = \left[G(U_1^{j+1}), G(U_2^{j+1}), \ldots, G(U_{N_x-1}^{j+1})\right]^T, \\ &f^{j+\sigma} = \left[f_1^{j+\sigma}, f_2^{j+\sigma}, \ldots, f_{N_x-1}^{j+\sigma}\right]^T, \quad \mathcal{E}^j = \varphi_0^j I_1 + \varphi_1^j I_2 + \varphi_{N_x-1}^j I_{N_x-1} + \varphi_{N_x}^j I_{N_x}, \\ &I_1 = [1,0,\ldots,0,0]^T, \ I_2 = [0,1,\ldots,0,0]^T, \ I_{N_x-1} = [0,0,\ldots,1,0]^T, \ I_{N_x} = [0,0,\ldots,0,1]^T, \\ &\varphi_0^j = -\left[\frac{\left(w_{j,j}^{(\alpha,\sigma)} + \sigma q^{j+\sigma}\right)}{12} - \frac{\sigma p^{j+\sigma}}{h_x^2}\right]\psi_1(t_{j+1}) - \frac{\sigma}{12}G(\psi_1(t_{j+1})) + \frac{1}{12}\sum_{i=1}^{j}\left(w_{j,i}^{(\alpha,\sigma)} - w_{j,i-1}^{(\alpha,\sigma)}\right) \\ &\quad \times \psi_1(t_i) + \frac{w_{j,0}^{(\alpha,\sigma)}}{12}\phi(x_0) - \frac{(1-\sigma)}{12}G(\psi_1(t_j)) + (1-\sigma)\left[\frac{p^{j+\sigma}}{h_x^2} - \frac{q^{j+\sigma}}{12}\right]\psi_1(t_j) + \frac{1}{12}f_0^{j+\sigma}, \\ &\varphi_1^j = -\left[\left(w_{j,j}^{(\alpha,\sigma)} + \sigma q^{j+\sigma}\right)\widetilde{p} - \frac{\sigma p^{j+\sigma}}{h_x^2}\mu\right]\psi_1(t_{j+1}) - \sigma\widetilde{p}G(\psi_1(t_{j+1})) + \widetilde{p}\sum_{i=1}^{j}\left(w_{j,i}^{(\alpha,\sigma)} - w_{j,i-1}^{(\alpha,\sigma)}\right) \\ &\quad \times \psi_1(t_i) + \widetilde{p}w_{j,0}^{(\alpha,\sigma)}\phi(x_0) - (1-\sigma)\widetilde{p}G(\psi_1(t_j)) + (1-\sigma)\left[\frac{p^{j+\sigma}}{h_x^2}\mu - \widetilde{p}q^{j+\sigma}\right]\psi_1(t_j) + \widetilde{p}f_0^{j+\sigma}, \end{aligned}$$

$$
\begin{aligned}
\varphi^{j}_{N_x-1} = &-\left[\left(w^{(\alpha,\sigma)}_{j,j} + \sigma q^{j+\sigma}\right)\widetilde{p} - \frac{\sigma p^{j+\sigma}}{h_x^2}\mu\right]\psi_2(t_{j+1}) - \sigma\widetilde{p}G(\psi_2(t_{j+1})) + \widetilde{p}\sum_{i=1}^{j}\left(w^{(\alpha,\sigma)}_{j,i} - w^{(\alpha,\sigma)}_{j,i-1}\right)\\
&\times \psi_2(t_i) + \widetilde{p}w^{(\alpha,\sigma)}_{j,0}\phi(x_0) - (1-\sigma)\widetilde{p}G(\psi_2(t_j)) + (1-\sigma)\left[\frac{p^{j+\sigma}}{h_x^2}\mu - \widetilde{p}q^{j+\sigma}\right]\psi_2(t_j) + \widetilde{p}f^{j+\sigma}_{N_x},\\
\varphi^{j}_{N_x} = &-\left[\frac{\left(w^{(\alpha,\sigma)}_{j,j} + \sigma q^{j+\sigma}\right)}{12} - \frac{\sigma p^{j+\sigma}}{h_x^2}\right]\psi_2(t_{j+1}) - \frac{\sigma}{12}G(\psi_2(t_{j+1})) + \frac{1}{12}\sum_{i=1}^{j}\left(w^{(\alpha,\sigma)}_{j,i} - w^{(\alpha,\sigma)}_{j,i-1}\right)\\
&\times \psi_2(t_i) + \frac{w^{(\alpha,\sigma)}_{j,0}}{12}\phi(x_0) - \frac{(1-\sigma)}{12}G(\psi_2(t_j)) + (1-\sigma)\left[\frac{p^{j+\sigma}}{h_x^2} - \frac{q^{j+\sigma}}{12}\right]\psi_2(t_j) + \frac{1}{12}f^{j+\sigma}_{N_x},
\end{aligned}
$$

and

$$
\mathcal{B} = \begin{pmatrix}
\frac{10}{12} & \frac{1}{12} & & & & & \\
\widetilde{q} & \widetilde{s} & \widetilde{q} & \widetilde{p} & & & \\
\widetilde{p} & \widetilde{q} & \widetilde{s} & \widetilde{q} & \widetilde{p} & & \\
 & & & \ddots & & & \\
 & & \widetilde{p} & \widetilde{q} & \widetilde{s} & \widetilde{q} & \widetilde{p} \\
 & & & \widetilde{p} & \widetilde{q} & \widetilde{s} & \widetilde{q} \\
 & & & & & \frac{1}{12} & \frac{10}{12}
\end{pmatrix}, \quad
\mathcal{K} = \begin{pmatrix}
-2 & 1 & & & & & \\
A_2 & A_3 & A_2 & A_1 & & & \\
A_1 & A_2 & A_3 & A_2 & A_1 & & \\
 & & & \ddots & & & \\
 & & A_1 & A_2 & A_3 & A_2 & A_1 \\
 & & & A_1 & A_2 & A_3 & A_2 \\
 & & & & & 1 & -2
\end{pmatrix},
$$

$A_1 = \mu$, $A_2 = (1-4\mu)$, $A_3 = (6\mu - 2)$.

5.2 Theoretical analysis

In this section, we examine the uniqueness of numerical solution, as well as the stability and convergence analysis of the developed fully discrete scheme (5.26).

To begin, we establish some notation and provide a set of lemmas that will serve as essential tools for our scheme analysis. For arbitrary $\bar{u}, \bar{v} \in \mathcal{D}^*_h$, we provide the definitions of the discrete inner product, $\mathcal{L}_2$ norm, H^1 semi-norm, and $\mathcal{L}_\infty$ norm as follows:

$$\langle \bar{u}, \bar{v} \rangle = h \sum_{m=1}^{N_x-1} \bar{u}_m \cdot \bar{v}_m, \qquad \|\bar{u}\| = \left(\langle \bar{u}, \bar{u} \rangle\right)^{1/2},$$
$$\|\delta_x \bar{u}\| = \left(h \sum_{m=1}^{N_x} \left(\delta_x \bar{u}_{m-\frac{1}{2}}\right)^2 \right)^{1/2}, \qquad \|\bar{u}\|_\infty = \max_{1 \le m \le N_x-1} |\bar{u}_m|.$$

Similarly, we can define $\|\delta_x^2 \bar{u}\|$ and $\|\mathcal{H}_q \bar{u}\|$.

Lemma 5.5. *Let's consider* $1 - \frac{\alpha}{2} \le \sigma \le 1$. *Under this condition, for any mesh function* $\{V_m^{j+1},\ 0 \le m \le N_x,\ 0 \le j \le N_t - 1\}$, *the following assertion holds true*

$$\|\mathcal{H}_q U^{j+1}\|^2 \le \|\mathcal{H}_q U^0\|^2 + \Gamma(1-\alpha) \max_{0 \le i \le j} \{t_{i+\sigma}^\alpha \Delta_t^\alpha \|\mathcal{H}_q U^{i+\sigma}\|^2\}, \ \textit{for}\ 0 \le j \le N_t - 1.$$

Proof. Assuming that $\max_{0 \le i \le j} \|\mathcal{H}_q U^{i+1}\|^2 = \|\mathcal{H}_q U^{k+1}\|^2$ is valid for a chosen $k \in \{0, \ldots, j\}$. It can be observed from Lemma 5.2 that $w_{k,k}^{(\alpha,\sigma)} > 0$ and $w_{k,i}^{(\alpha,\sigma)} > w_{k,i-1}^{(\alpha,\sigma)}$ for all k and i. Set $\mathcal{W}^i = \|\mathcal{H}_q U^i\|^2 - \|\mathcal{H}_q U^0\|^2$ for all i. As $\Delta_t^\alpha \|\mathcal{H}_q U^0\|^2 = 0$, we have

$$\begin{aligned}
\Delta_t^\alpha \|\mathcal{H}_q U^{k+\sigma}\|^2 = \Delta_t^\alpha \mathcal{W}^{k+\sigma} &= w_{k,k}^{(\alpha,\sigma)} \mathcal{W}^{k+1} - \sum_{i=1}^{k} \left(w_{k,i}^{(\alpha,\sigma)} - w_{k,i-1}^{(\alpha,\sigma)} \right) \mathcal{W}^i \\
&\ge w_{k,k}^{(\alpha,\sigma)} \mathcal{W}^{k+1} - \sum_{i=1}^{k} \left(w_{k,i}^{(\alpha,\sigma)} - w_{k,i-1}^{(\alpha,\sigma)} \right) \left(\|\mathcal{H}_q U^{k+1}\|^2 - \|\mathcal{H}_q U^0\|^2 \right) \\
&= w_{k,0}^{(\alpha,\sigma)} \left(\|\mathcal{H}_q U^{k+1}\|^2 - \|\mathcal{H}_q U^0\|^2 \right).
\end{aligned}$$

Which on solving gives

$$\|\mathcal{H}_q U^{k+1}\|^2 \le \|\mathcal{H}_q U^0\|^2 + \left(w_{k,0}^{(\alpha,\sigma)} \right)^{-1} \Delta_t^\alpha \|\mathcal{H}_q U^{k+\sigma}\|^2.$$

The result follows from Lemma 5.2. □

Lemma 5.6. *[100] Let* $\vartheta \in \mathcal{D}_h^*$. *If* $\mu \in \left(0, \frac{67}{492}\right)$, *then*

$$\xi_0^2 \langle \vartheta, \vartheta \rangle \leq \langle \mathcal{H}_q \vartheta, \mathcal{H}_q \vartheta \rangle \leq \left(\frac{61}{60}\right)^2 \langle \vartheta, \vartheta \rangle, \tag{5.27}$$

where $\xi_0 > 0$ *is given by*

$$\xi_0 = \begin{cases} -\frac{71\mu}{24} + \frac{283}{480}, & 0 < \mu \leq \frac{1}{20}, \\ -\frac{9\mu}{2} + \frac{2}{3}, & \mu = \frac{1}{20}, \\ -\frac{41\mu}{8} + \frac{67}{96}, & \frac{1}{20} < \mu < \frac{67}{492}. \end{cases}$$

Lemma 5.7. *[100] Let* $\vartheta \in \mathcal{D}_h^*$. *If* $\mu \in (0, \tilde{\mu}_0)$, *where* $\tilde{\mu}_0 = \frac{-161+12\sqrt{229}}{340}$ (≈ 0.06), *then*

$$\left\langle \mathcal{H}_q \vartheta, \tilde{\delta}_x^2 \vartheta \right\rangle \leq -\frac{4\xi_1}{(b-a)} \langle \vartheta, \vartheta \rangle, \tag{5.28}$$

where $\xi_1 > 0$ *is given by*

$$\xi_1 = \begin{cases} \frac{71}{120} - 7\mu + 18\mu^2, & 0 < \mu < \tilde{\mu}_1, \\ \frac{2}{3} - 10\mu, & \mu = \tilde{\mu}_1, \\ \frac{83}{120} - 11\mu - 6\mu^2, & \tilde{\mu}_1 < \mu \leq \frac{1}{20}, \\ \frac{83}{120} - \frac{1288\mu}{120} - \frac{1360\mu^2}{120}, & \frac{1}{20} < \mu < \tilde{\mu}_0. \end{cases}$$

Here, $\tilde{\mu}_0 = \frac{-161+12\sqrt{229}}{340}$ *and* $\tilde{\mu}_1 = \frac{-5+2\sqrt{10}}{60}$.

5.2.1 Uniqueness of the numerical solution

Theorem 5.2. *The solution* $\{U_m^j,\ 0 \leq m \leq N_x,\ 0 \leq j \leq N_t\}$ *obtained by the fully discrete scheme (5.25) is unique.*

Proof. Assuming U_m^j and V_m^j both satisfy scheme (5.25) under the same initial and boundary conditions, let $\zeta_m^j = U_m^j - V_m^j$. It is evident that $\zeta_m^i \in \mathcal{D}_h^*$ and satisfies the subsequent equation

$$\Delta_t^\alpha \mathcal{H}_q \zeta_m^{j+\sigma} - p^{j+\sigma}\tilde{\delta}_x^2 \zeta_m^{j,\sigma} + q^{j+\sigma}\mathcal{H}_q \zeta_m^{j,\sigma} + \Big(\mathcal{H}_q G(U_m^{j,\sigma}) - \mathcal{H}_q G(V_m^{j,\sigma})\Big) = 0, \tag{5.29}$$

with initial and boundary conditions

$$\begin{cases} \zeta_m^0 = 0, & 0 \le m \le N_x, \\ \zeta_0^j = \zeta_{N_x}^j = 0, & 1 \le j \le N_t. \end{cases} \tag{5.30}$$

Upon multiplication of Equation (5.29) by $h\mathcal{H}_q\zeta_m^{j,\sigma}$ and then summing from $m = 1$ to $N_x - 1$, then outcome is as follows

$$\begin{aligned} \langle \Delta_t^\alpha \mathcal{H}_q \zeta^{j+\sigma}, \mathcal{H}_q \zeta^{j,\sigma}\rangle - p^{j+\sigma}\langle \tilde{\delta}_x^2 \zeta^{j,\sigma}, \mathcal{H}_q \zeta^{j,\sigma}\rangle + q^{j+\sigma}\langle \mathcal{H}_q \zeta^{j,\sigma}, \mathcal{H}_q \zeta^{j,\sigma}\rangle \\ + \Big\langle \Big(\mathcal{H}_q G(U_m^{j,\sigma}) - \mathcal{H}_q G(V_m^{j,\sigma})\Big), \mathcal{H}_q \zeta^{j,\sigma} \Big\rangle = 0. \end{aligned} \tag{5.31}$$

Following the same line of reasoning as demonstrated in [7, Lemma 1], it can be affirmed that

$$\langle \Delta_t^\alpha \mathcal{H}_q \zeta^{j+\sigma}, \mathcal{H}_q \zeta^{j,\sigma}\rangle \ge \frac{1}{2}\Delta_t^\alpha \|\mathcal{H}_q \zeta^{j+\sigma}\|^2. \tag{5.32}$$

Moreover, with the utilization of Lemma 5.7, it becomes apparent that

$$\langle \tilde{\delta}_x^2 \zeta^{j,\sigma}, \mathcal{H}_q \zeta^{j,\sigma}\rangle \le -\frac{4\xi_1}{(b-a)}\|\zeta^{j,\sigma}\|^2. \tag{5.33}$$

By invoking the mean value theorem of differential calculus and considering the condition $G(0) = 0$, we obtain

$$\left\langle \left(\mathcal{H}_q G(U_m^{j,\sigma}) - \mathcal{H}_q G(V_m^{j,\sigma})\right), \mathcal{H}_q \zeta^{j,\sigma} \right\rangle = G'(c)\|\mathcal{H}_q \zeta^{j,\sigma}\|^2. \tag{5.34}$$

Upon incorporating the inequalities (5.32), (5.33), and (5.34) into equation (5.31), we find that

$$\frac{1}{2}\Delta_t^{\alpha}\|\mathcal{H}_q \zeta^{j+\sigma}\|^2 + c_1 \frac{4\xi_1}{(b-a)}\|\zeta^{j,\sigma}\|^2 + \left(G'(c) + c_2\right)\|\mathcal{H}_q \zeta^{j,\sigma}\|^2 \leq 0,$$

this implies that

$$\Delta_t^{\alpha}\|\mathcal{H}_q \zeta^{j+\sigma}\|^2 \leq 0. \tag{5.35}$$

Furthermore, by virtue of Lemma 5.5 and considering the condition $\zeta^0 = 0$, it follows that

$$\begin{aligned} \|\mathcal{H}_q \zeta^{j+1}\|^2 &\leq \|\mathcal{H}_q \zeta^0\|^2 + \Gamma(1-\alpha) \max_{0 \leq i \leq j}\{t_{i+\sigma}^{\alpha} \Delta_t^{\alpha}\|\mathcal{H}_q \zeta^{i+\sigma}\|^2\} \\ &= \Gamma(1-\alpha) \max_{0 \leq i \leq j}\{t_{i+\sigma}^{\alpha} \Delta_t^{\alpha}\|\mathcal{H}_q \zeta^{i+\sigma}\|^2\} \leq \ 0. \end{aligned}$$

In addition, by invoking Lemma 5.6, we get

$$\xi_0^2\|\zeta^{j+1}\|^2 \leq \|\mathcal{H}_q \zeta^{j+1}\|^2 \leq 0.$$

Hence, we can conclude that $\zeta_m^j = U_m^j - V_m^j = 0$, which implies that $U_m^j = V_m^j$. This validates the intended outcome. □

5.2.2 Stability analysis

Let ε_m^j be the solution to the following problem

$$\Delta_t^\alpha \mathcal{H}_q \varepsilon_m^{j+\sigma} - p^{j+\sigma}\tilde{\delta}_x^2 \varepsilon_m^{j,\sigma} + q^{j+\sigma}\mathcal{H}_q \varepsilon_m^{j,\sigma} + \Big(\mathcal{H}_q G(\varepsilon_m^{j,\sigma}) - \mathcal{H}_q G(U_m^{j,\sigma})\Big) = \mathcal{H}_q \hat{f}_m^{j+\sigma},$$
$$1 \leq m \leq N_x - 1,\ 0 \leq j \leq N_t - 1. \tag{5.36}$$

with initial and boundary conditions

$$\begin{cases} \varepsilon_m^0 = \tilde{\phi}(x_m), & 0 \leq m \leq N_x, \\ \varepsilon_0^j = \psi_1(t_j), & 1 \leq j \leq N_t, \\ \varepsilon_{N_x}^j = \psi_2(t_j), & 1 \leq j \leq N_t. \end{cases} \tag{5.37}$$

Now, define $\varrho_m^j = \varepsilon_m^j - U_m^j$. It becomes evident, based on equations (5.36)-(5.37) and (5.25)-(5.23), that ϱ_j^j belongs to $\mathcal{D}_h^*$ and serves as the solution to the subsequent system

$$\Delta_t^\alpha \mathcal{H}_q \varrho_m^{j+\sigma} - p^{j+\sigma}\tilde{\delta}_x^2 \varrho_m^{j,\sigma} + q^{j+\sigma}\mathcal{H}_q \varrho_m^{j,\sigma} + \Big(\mathcal{H}_q G(\varepsilon_m^{j,\sigma}) - \mathcal{H}_q G(U_m^{j,\sigma})\Big) = \mathcal{H}_q \bar{f}_m^{j+\sigma},$$
$$1 \leq m \leq N_x - 1,\ 0 \leq j \leq N_t - 1. \tag{5.38}$$

with initial and boundary conditions

$$\begin{cases} \varrho_m^0 = \tilde{\phi}(x_m) - \phi(x_m), & 0 \leq m \leq N_x, \\ \varrho_0^j = 0, & 1 \leq j \leq N_t, \\ \varrho_{N_x}^j = 0, & 1 \leq j \leq N_t. \end{cases} \tag{5.39}$$

where $\bar{f}_m^{j+\sigma} = \hat{f}_m^{j+\sigma} - f_m^{j+\sigma}$. Our next step involves proving a result that directly confirms the scheme's stability.

Theorem 5.3. *The solution to the discrete problem (5.38)-(5.39) satisfies*

$$\|\varrho^{j+1}\|^2 \leq \frac{1}{\xi_0^2}\left[\|\mathcal{H}_q\varrho^0\|^2 + \frac{(b-a)\Gamma(1-\alpha)T^\alpha}{8c_1\xi_1}\left(\frac{61}{60}\right)^2 \max_{0\leq i\leq j}\|\mathcal{H}_q\bar{f}^{i+\sigma}\|^2\right],$$

where ξ_0, ξ_1, and c_1 are positive constants.

Proof. Upon multiplication of Equation (5.38) by $h\mathcal{H}_q\varrho_m^{j,\sigma}$ and then summing from $m=1$ to N_x-1, then outcome is as follows

$$\begin{aligned}&\langle\Delta_t^\alpha\mathcal{H}_q\varrho^{j+\sigma},\mathcal{H}_q\varrho^{j,\sigma}\rangle - p^{j+\sigma}\langle\tilde{\delta}_x^2\varrho^{j,\sigma},\mathcal{H}_q\varrho^{j,\sigma}\rangle + q^{j+\sigma}\langle\mathcal{H}_q\varrho^{j,\sigma},\mathcal{H}_q\varrho^{j,\sigma}\rangle\\ &\quad+\left\langle\Big(\mathcal{H}_qG(\varepsilon^{j,\sigma})-\mathcal{H}_qG(U^{j,\sigma})\Big),\mathcal{H}_q\varrho^{j,\sigma}\right\rangle = \langle\mathcal{H}_q\bar{f}^{j+\sigma},\mathcal{H}_q\varrho^{j,\sigma}\rangle.\end{aligned} \tag{5.40}$$

Following the same line of reasoning as demonstrated in [7, Lemma 1], it can be affirmed that

$$\langle\Delta_t^\alpha\mathcal{H}_q\varrho^{j+\sigma},\mathcal{H}_q\varrho^{j,\sigma}\rangle \geq \frac{1}{2}\Delta_t^\alpha\|\mathcal{H}_q\varrho^{j+\sigma}\|^2. \tag{5.41}$$

Moreover, with the utilization of Lemma 5.7, it becomes apparent that

$$\langle\tilde{\delta}_x^2\varrho^{j,\sigma},\mathcal{H}_q\varrho^{j,\sigma}\rangle \leq -\frac{4\xi_1}{(b-a)}\|\varrho^{j,\sigma}\|^2. \tag{5.42}$$

By invoking the mean value theorem of differential calculus and considering the condition $G(0)=0$, we obtain

$$\left\langle\Big(\mathcal{H}_qG(\varepsilon_m^{j,\sigma})-\mathcal{H}_qG(U_m^{j,\sigma})\Big),\mathcal{H}_q\varrho^{j,\sigma}\right\rangle = G'(c)\|\mathcal{H}_q\varrho^{j,\sigma}\|^2. \tag{5.43}$$

Furthermore, for any positive ϵ, applying Young's inequality and utilizing Lemma 5.6 on the term $\langle \mathcal{H}_q \bar{f}^{j+\sigma}, \mathcal{H}_q \varrho^{j,\sigma}\rangle$ results in

$$\langle \mathcal{H}_q \bar{f}^{j+\sigma}, \mathcal{H}_q \varrho^{j,\sigma}\rangle \leq \epsilon \|\mathcal{H}_q \varrho^{j,\sigma}\|^2 + \frac{1}{4\epsilon}\|\mathcal{H}_q \bar{f}^{j+\sigma}\|^2 \leq \epsilon \left(\frac{61}{60}\right)^2 \|\varrho^{j,\sigma}\|^2 + \frac{1}{4\epsilon}\|\mathcal{H}_q \bar{f}^{j+\sigma}\|^2. \tag{5.44}$$

With ϵ being assigned a value of $c_1 \frac{4\xi_1}{(b-a)} \left(\frac{60}{61}\right)^2$, the utilization of inequalities (5.41), (5.42), (5.43), and (5.44) in equation (5.40) leads to the following outcome

$$\begin{aligned}\frac{1}{2}\Delta_t^{\alpha}\|\mathcal{H}_q \varrho^{j+\sigma}\|^2 + c_1 \frac{4\xi_1}{(b-a)}\|\varrho^{j,\sigma}\|^2 + \left(G'(c) + c_2\right)\|\mathcal{H}_q \varrho^{j,\sigma}\|^2 \\ \leq \; c_1 \frac{4\xi_1}{(b-a)}\|\varrho^{j,\sigma}\|^2 + \frac{(b-a)}{16 c_1 \xi_1}\left(\frac{61}{60}\right)^2 \|\mathcal{H}_q \bar{f}^{j+\sigma}\|^2,\end{aligned}$$

which gives

$$\Delta_t^{\alpha}\|\mathcal{H}_q \varrho^{j+\sigma}\|^2 \leq \frac{(b-a)}{8 c_1 \xi_1}\left(\frac{61}{60}\right)^2 \|\mathcal{H}_q \bar{f}^{j+\sigma}\|^2.$$

Additionally, by virtue of Lemma 5.5, we arrive at the following

$$\|\mathcal{H}_q \varrho^{j+1}\|^2 \leq \|\mathcal{H}_q \varrho^{0}\|^2 + \frac{(b-a)\Gamma(1-\alpha)T^{\alpha}}{8 c_1 \xi_1}\left(\frac{61}{60}\right)^2 \max_{0\leq i\leq j}\|\mathcal{H}_q \bar{f}^{i+\sigma}\|^2.$$

Furthermore, the theorem follows directly from the application of Lemma 5.6. $\square$

5.2.3 Convergence analysis

In this section, our objective is to discuss the convergence of the scheme outlined in equation (5.25).

Theorem 5.4. *Assume that the problem (5.1)-(5.2) has the solution $u(x,t)$, which meets the assumptions provided in (5.3) and (5.4) and let $\{U_m^i \mid 0 \leq m \leq N_x, 0 \leq$*

$i \leq N_t\}$ be the solution of the fully discrete scheme given by (5.25). Then we have

$$\max_{0\leq i\leq N_t-1} \|u^{i+1} - U^{i+1}\|_2 \leq c\left(N_t^{-\min\{\theta\alpha,2\}} + h^{4.5}\right),$$

where c is a positive constant independent of N_t and N_x.

Proof. By subtracting (5.25) from (5.24), we obtain

$$\Delta_t^{\alpha}\mathcal{H}_q e_m^{j+\sigma} - p^{j+\sigma}\tilde{\delta}_x^2 e_m^{j,\sigma} + q^{j+\sigma}\mathcal{H}_q e_m^{j,\sigma} + \left(\mathcal{H}_q G(u_m^{j,\sigma}) - \mathcal{H}_q G(U_m^{j,\sigma})\right) = \mathcal{R}_f,$$
$$1 \leq m \leq N_x - 1,\ 0 \leq j \leq N_t - 1. \qquad (5.45)$$

with initial and boundary conditions

$$\begin{cases} e_m^0 = 0, & 0 \leq m \leq N_x, \\ e_0^j = 0, & 1 \leq j \leq N_t, \\ e_{N_x}^j = 0, & 1 \leq j \leq N_t, \end{cases} \qquad (5.46)$$

where $e_m^j = u_m^j - U_m^j$. It becomes evident that $e_m^j \in \mathcal{D}_h^*$.

By applying the operation of multiplication to equation (5.45) with $h\mathcal{H}_q e_m^{i,\sigma}$, followed by summation over m ranging from 1 to $N_x - 1$, we obtain the following outcome

$$\langle \Delta_t^{\alpha}\mathcal{H}_q e^{j+\sigma}, \mathcal{H}_q e^{j,\sigma}\rangle - p^{j+\sigma}\langle \tilde{\delta}_x^2 e^{j,\sigma}, \mathcal{H}_q e^{j,\sigma}\rangle + q^{j+\sigma}\langle \mathcal{H}_q e^{j,\sigma}, \mathcal{H}_q e^{j,\sigma}\rangle$$
$$+\left\langle \left(\mathcal{H}_q G(u^{j,\sigma}) - \mathcal{H}_q G(U^{j,\sigma})\right), \mathcal{H}_q e^{j,\sigma}\right\rangle = \langle \mathcal{R}_f, \mathcal{H}_q e^{j,\sigma}\rangle. \qquad (5.47)$$

By using inequality (5.32), Lemma 5.7 and the mean value theorem of differential calculus under the condition $G(0) = 0$, and coefficients $p(t)$ and $q(t)$ being bounded, it holds

$$\frac{1}{2}\Delta_t^{\alpha}\|\mathcal{H}_q e^{j+\sigma}\|^2 + c_1\frac{4\xi_1}{(b-a)}\|e^{j,\sigma}\|^2 + (G'(c)+c_2)\,\|\mathcal{H}_q e^{j,\sigma}\|^2 \leq \langle \mathcal{R}_f, \mathcal{H}_q e^{j,\sigma}\rangle.$$

Expanding further through the application of the Cauchy-Schwarz inequality and Lemma 5.6, we obtain

$$\Delta_t^{\alpha}\|\mathcal{H}_q e^{j+\sigma}\|^2 \leq 2\|\mathcal{R}_f\|\|\mathcal{H}_q e^{j,\sigma}\| \leq 2\left(\frac{61}{60}\right)\|\mathcal{R}_f\|\|e^{j,\sigma}\| \leq c\|\mathcal{R}_f\|\max_{0\leq j\leq N_t-1}\|e^{j+1}\|, \tag{5.48}$$

where $c = (61/30)$. Additionally, when we take into account Lemma 5.5, Lemma 5.6, and the fact that $\|\mathcal{H}_q e^0\| = 0$, then the following inequality holds for $0 \leq j \leq N_t - 1$

$$\xi_0^2\|e^{j+1}\|^2 \leq \|\mathcal{H}_q e^{j+1}\|^2 \leq c\Gamma(1-\alpha)\max_{0\leq j\leq N_t-1}\{t_{j+\sigma}^{\alpha}\|\mathcal{R}_f\|\}\max_{0\leq j\leq N_t-1}\|e^{j+1}\|.$$

It follows that

$$\max_{0\leq j\leq N_t-1}\|e^{j+1}\|^2 \leq \frac{c\Gamma(1-\alpha)}{\xi_0^2}\max_{0\leq j\leq N_t-1}\{t_{j+\sigma}^{\alpha}\|\mathcal{R}_f\|\}\max_{0\leq j\leq N_t-1}\|e^{j+1}\|.$$

Thus, we get

$$\max_{0\leq j\leq N_t-1}\|e^{j+1}\| \leq \frac{c\Gamma(1-\alpha)}{\xi_0^2}\max_{0\leq j\leq N_t-1}\{t_{j+\sigma}^{\alpha}\|\mathcal{R}_f\|\}.$$

Furthermore, by utilizing the expression for $\mathcal{R}_f$, we obtain

$$\max_{0\leq j\leq N_t-1}\|e^{j+1}\| \leq \frac{c\Gamma(1-\alpha)}{\xi_0^2}\big[\mathcal{N}_1 + \mathcal{N}_2 + \mathcal{N}_3\big]. \tag{5.49}$$

where $\mathcal{N}_1 = \max_{0\leq j\leq N_t-1} t_{j+\sigma}^{\alpha}\|\mathcal{R}_t^{j+\sigma}\|$, $\mathcal{N}_2 = \max_{0\leq j\leq N_t-1} t_{j+\sigma}^{\alpha}\|(\mathcal{R}_t^{\alpha})^{j,\sigma}\|$, and
$\mathcal{N}_3 = \max_{0\leq j\leq N_t-1} t_{j+\sigma}^{\alpha}\|\mathcal{R}_x\|$.

Further, by employing Lemma 5.1 within the expression for $\mathcal{N}_1$, we get

$$\mathcal{N}_1 \leq cN_t^{-\min\{3-\alpha,\theta\alpha\}}. \tag{5.50}$$

Next, we proceed to estimate the term $\mathcal{N}_2 = \max_{0\leq j\leq N_t-1} t_{j+\sigma}^{\alpha}\|(\mathcal{R}_t^{\alpha})^{j,\sigma}\|$. When $j = 0$, under the assumption that $\|u(t)\|_2 \leq c$, we find that $t_{\sigma}^{\alpha}\|(\mathcal{R}_t^{\alpha})^{0,\sigma}\| \leq ct_{\sigma}^{\alpha} \leq ct_1^{\alpha} \leq cN_t^{-\theta\alpha}$ (as $t_1 \leq cN_t^{-\theta}$). Furthermore, with the aid of Lemma 5.3 and under the prescribed conditions: $t_{j+1} \leq 2^{\theta}t_j$ for $j = 1, \ldots, N_t - 1$, $\Delta t_{j+1} \leq T^{1/\theta}N_t^{-1}t_{j+1}^{1-1/\theta}$ for $j = 1, \ldots, N_t$, and $t_1 \leq cN_t^{-\theta}$, and assuming the hypothesis $\|\partial_t^2 u(t)\|_2 \leq c(1 + t^{\alpha-2})$ we can establish the following for $j = 1, \ldots, N_t$

$$\begin{aligned}
t_{j+\sigma}^{\alpha}\|(\mathcal{R}_t^{\alpha})^{j,\sigma}\| &\leq \frac{1}{8}t_{j+\sigma}^{\alpha}\Delta t_{j+1}^2 \max_{\tau\in(t_j,t_{j+1})} |\partial_\tau^2 u(\tau)| \leq ct_{j+1}^{\alpha}\Delta t_{j+1}^2 t_j^{\alpha-2} \leq cN_t^{-2}t_{j+1}^{2\theta-2/\theta} \\
&\leq \begin{cases} cN_t^{-2}t_1^{2\theta-2/\theta} \leq cN_t^{-2\theta\alpha}, & 1 \leq \theta \leq 1/\alpha, \\ cN_t^{-2}, & \theta \geq 1/\alpha. \end{cases}
\end{aligned}$$

Thus, we get

$$\mathcal{N}_2 = \max_{0\leq j\leq N_t-1} t_{j+\sigma}^{\alpha}\|(\mathcal{R}_t^{\alpha})^{j,\sigma}\| \leq cN_t^{-\min\{\theta\alpha,2\}}. \tag{5.51}$$

Furthermore, we move forward with the assessment of the term $\mathcal{N}_3$, making use of the Lemma 5.4.

$$\begin{aligned}
\mathcal{N}_3 = &\max_{0\leq j\leq N_t-1} t_{j+\sigma}^{\alpha}\|\mathcal{R}_x\| \leq T^{\alpha}\|\mathcal{R}_x\| \\
=&T^{\alpha}\left[h\sum_{m=1}^{N_x-1}(\mathcal{R}_x)^2\right]^{1/2} \\
\leq&T^{\alpha}\left[2h\left(h^4\right)^2 + h(N_x-3)\left(h^6\right)^2\right]^{1/2} \\
\leq&T^{\alpha}\left[2\left(h^{4.5}\right)^2 + (b-a)\left(h^6\right)^2\right]^{1/2}
\end{aligned}$$

$$\leq T^{\alpha}\Big(2+(b-a)h^{3}\Big)^{1/2}h^{4.5}.$$

Thus

$$\mathcal{N}_3 \leq c\ h^{4.5}. \tag{5.52}$$

Now, by applying the inequalities (5.50), (5.51), and (5.52) to inequality (5.49), we obtain the theorem

$$\max_{0\leq j\leq N_t-1}\|e^{j+1}\| \leq c\ \left(N_t^{-\min\{\theta\alpha,2\}} + h^{4.5}\right). \tag{5.53}$$

□

Remark 5.5. It is apparent from the error inequality (5.53) that our numerical scheme (5.25) represents an improvement over both the compact finite difference method, which achieves a spatial convergence order of $\mathcal{O}(h^4)$ (the best achieved so far), and the finite difference method, which reaches a spatial convergence order of $\mathcal{O}(h^2)$ for a non-linear time-fractional reaction-diffusion equation with variable coefficients.

Remark 5.6. Convergence analysis in Theorem 5.4 establishes a spatial convergence order of $\mathcal{O}(h^{4.5})$. In practice, it is noteworthy that we might attain a higher spatial convergence order, especially for certain problem types. This fact is clearly demonstrated through the numerical experiments outlined in Section 5.3.

5.3 Numerical results

This section is dedicated to presenting the outcomes of a comprehensive numerical illustration, designed to assess the practical implementation of the proposed numerical method. To assess the accuracy of the numerical solution, we compare the exact solution $u(x_m, t_j)$ and the approximate solution $U(x_m, t_j)$ of the problem (5.1)-(5.2) at (x_m, t_j) using the following norms

$$\mathcal{L}_\infty(h, \Delta t) = \|u - U\|_\infty = \max_{1\le j\le N_t} \max_{1\le m\le N_x} |u(x_m, t_j) - U(x_m, t_j)|, \tag{5.54}$$

$$\mathcal{L}_2(h, \Delta t) = \|u - U\|_2 = \max_{1\le j\le N_t} \left[h \sum_{m=1}^{N_x-1} (u(x_m, t_j) - U(x_m, t_j))^2 \right]^{1/2}. \tag{5.55}$$

The evaluation of convergence order is conducted using the following formula

$$cov.order = \begin{cases} log_2 \left(\frac{\mathcal{L}_l(h,\Delta t_1)}{\mathcal{L}_l(h,\Delta t_2)} \right), & \text{in time,} \\ log_2 \left(\frac{\mathcal{L}_l((h)_1,\Delta t)}{\mathcal{L}_l((h)_2,\Delta t)} \right), & \text{in space,} \end{cases} \tag{5.56}$$

where $l = 2$ or ∞.

Newton's iterative technique to address non-linear reaction term

The non-linear function $G(u)$ in terms of the variable u leads to the emergence of equation (5.26) as a system of non-linear algebraic equations. Confronted with this complexity, the utilization of conventional linearization techniques becomes impractical. Instead, the employment of a specialized non-linear solver becomes essential. Notably, the Newton-Raphson iterative algorithm emerges as the method of choice due to its rapid convergence and uncomplicated implementation. In order to implement Newton's method, we derive the subsequent iterative representation from equation (5.26)

$$\mathcal{A}^j U^{[j+1,l+1]} + \sigma \mathcal{B} G\left(U^{[j+1,l+1]}\right) = w_{j,0}^{(\alpha,\sigma)} \mathcal{B} U^0 + \sum_{i=1}^{j} \left(w_{j,i}^{(\alpha,\sigma)} - w_{j,i-1}^{(\alpha,\sigma)} \right) \mathcal{B} U^i + \mathcal{D}^j U^j \\ - (1-\sigma)\mathcal{B} G(U^j) + \mathcal{B} f^{j+\sigma} + \mathcal{E}^j, \; 0 \le j \le N_t - 1, \; d \ge 0. \tag{5.57}$$

By implementing Newton's method to the term $G(U^{[j+1,l+1]})$, we arrive at

$$G\left(U^{[j+1,l+1]}\right) = G\left(U^{[j+1,l]}\right) + \left(U^{[j+1,l+1]} - U^{[j+1,l]}\right) G'\left(U^{[j+1,l]}\right). \tag{5.58}$$

Upon plugging in equation (5.58) into equation (5.57), we derive the subsequent Newton's iterative formula

$$\left[\mathcal{A}^j + \sigma\hat{D}\left(\mathcal{B}.G'\left(U^{[j+1,l]}\right)\right)\right] U^{[j+1,l+1]} = \sigma\hat{D}\left(\mathcal{B}.G'\left(U^{[j+1,l]}\right)\right) U^{[j+1,l]} - \sigma\mathcal{B} \times G\left(U^{[j+1,l]}\right) + \mathcal{M}^j, \tag{5.59}$$

where

$$\mathcal{M}^j = w_{j,0}^{(\alpha,\sigma)}\mathcal{B}U^0 + \sum_{i=1}^{j}\left(w_{j,i}^{(\alpha,\sigma)} - w_{j,i-1}^{(\alpha,\sigma)}\right)\mathcal{B}U^i + \mathcal{D}^j U^j - (1-\sigma)\mathcal{B}G(U^j) + \mathcal{B}f^{j+\sigma} + \mathcal{E}^j,$$

$U^{[j,l]}$ represents the value attained from the lth step iteration at the jth time level, and the notation $\hat{D}$ is applied for the purpose of transforming the vector into a diagonal matrix.

Remark 5.7. In order to avoid inaccuracies due to roundoff, we utilize adaptive Gauss-Kronrod quadrature (based on the methodology from [69]) for the computation of coefficients $r_{j,i}^{(\alpha,\sigma)}$ and $s_{j,i}^{(\alpha,\sigma)}$ in equations (5.9) and (5.10).

Example 5.1. *Let's consider the following non-linear TFRDE with variable coefficients*

$${}_0^C D_t^\alpha u(x,t) - t^2\frac{\partial^2 u(x,t)}{\partial x^2} + tu(x,t) + \left(\frac{u}{2} - \frac{\sin 2u}{4}\right)(x,t) = f(x,t),\ (x,t) =: (0,1)\times(0,1],$$

with initial and boundary conditions

$$\begin{cases} u(x,0) = \sin \pi x, & x \in [0,1], \\ u(0,t) = u(1,t) = 0, & t \in (0,1], \end{cases}$$

where

$$f(x,t) = \Gamma(1+\alpha)\sin(\pi x) + (\pi^2 t^2 + t + 1/2)(1+t^\alpha)\sin(\pi x) - \frac{\sin\big(2(1+t^\alpha)\sin \pi x\big)}{4}.$$

The exact solution is $u(x,t) = (1+t^\alpha)\sin \pi x$.

We have executed the implementation of the proposed scheme (5.25) on this test example, exploring different values of the fractional order α, along with varying discretization parameters N_x and N_t.

The temporal order of convergence, with respect to both the $\mathcal{L}_\infty$ and $\mathcal{L}_2$ norms, is summarized in Tables 5.1, 5.2, 5.3, and 5.4. In Tables 5.1 and 5.2, the temporal convergence orders, taking into account $\alpha = 0.1$ and $\alpha = 0.9$, respectively, for different grading parameters, including $\theta = 1, \frac{1}{\alpha}, \frac{2}{\alpha}$, and $\frac{3-\alpha}{\alpha}$ have been provided. Upon reviewing these tables, an interesting observation emerges. Specifically, when examining the temporal order of convergence with $\theta = 1$ (indicating uniform spacing), it becomes evident that the achieved convergence order is below α. This discrepancy can be attributed to the inherent characteristics of the solution to the problem, which displays a weak singularity at $t = 0$. Furthermore, by employing a graded mesh with different grading parameters, it has been noticed that $\theta = \frac{2}{\alpha}$ exhibits optimal grading characteristics. Therefore, in Table 5.3, we have provided the temporal order of convergence with $\theta = \frac{2}{\alpha}$ for various α values $(0.2, 0.4, 0.6, 0.8)$. Additionally, in Table 5.4, we provide a detailed comparison between our proposed method and the approach outlined in [91]. It is noteworthy that despite [91] being specifically

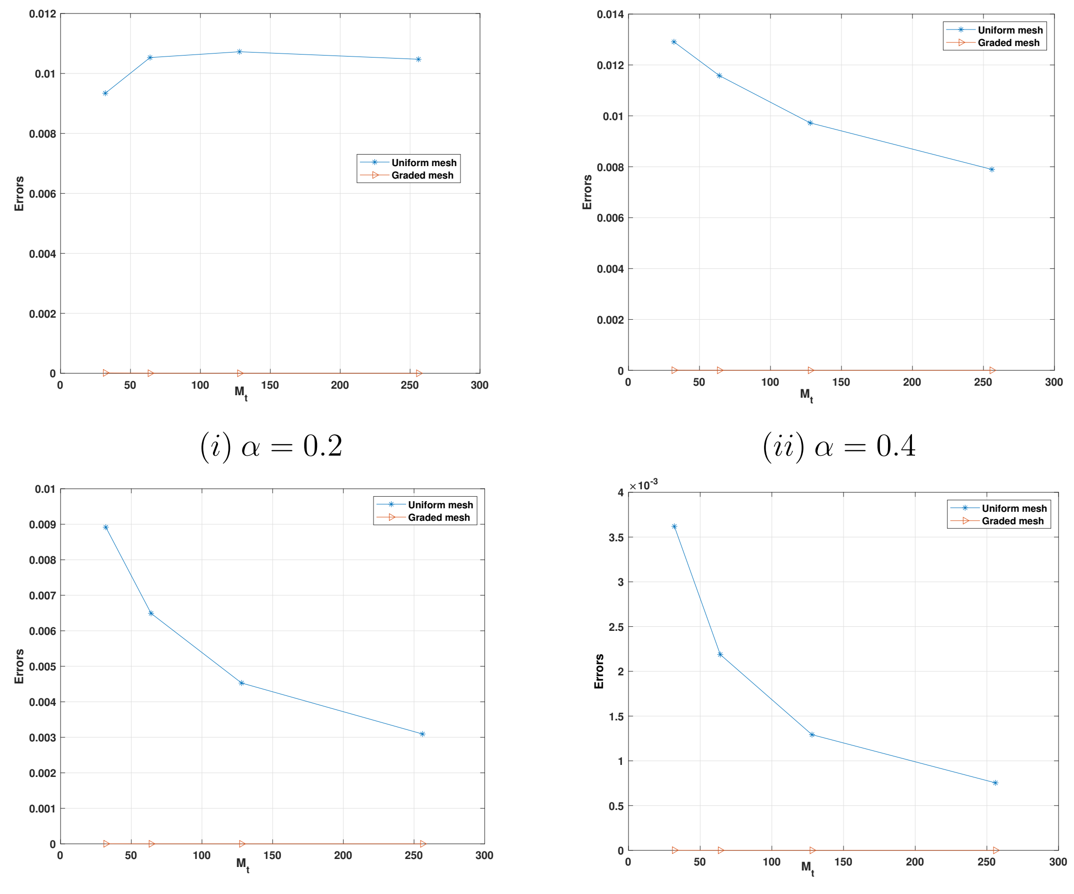

$(i)\ \alpha = 0.2$ $(ii)\ \alpha = 0.4$

$(iii)\ \alpha = 0.6$ $(iv)\ \alpha = 0.8$

FIGURE 5.1: $\mathcal{L}_2$-error using uniform and graded meshes for different values of α with $N_x = N_t$.

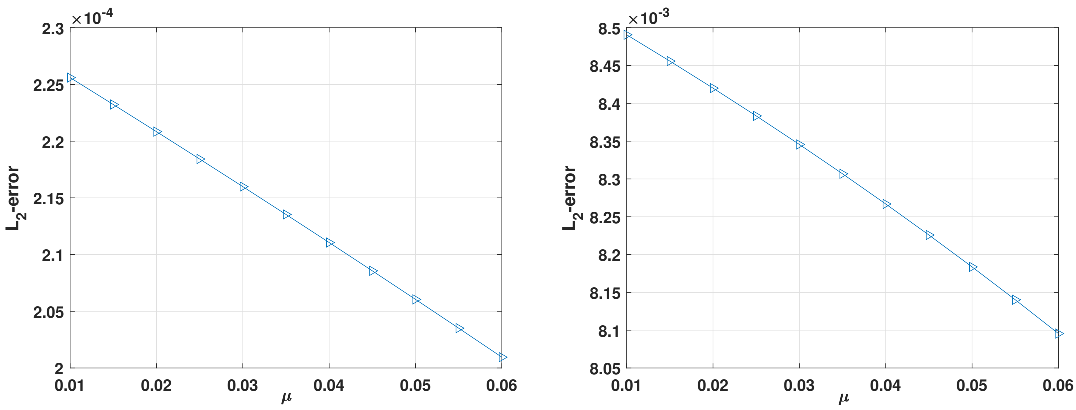

(a) Example 5.1 (b) Example 5.2

FIGURE 5.2: $\mathcal{L}_2\left(\frac{1}{5}, \frac{1}{250}\right)$ for various μ with $\alpha = 0.8$.

TABLE 5.1: (Example 5.1) $\mathcal{L}_\infty$ and $\mathcal{L}_2$ errors with temporal order of convergence for $\alpha = 0.1$.

θ	$N_x = N_t$	$\mathcal{L}_\infty$-error	cov.order$_t$	$\mathcal{L}_2$-error	cov.order$_t$	Optimal order
1	64	7.4965e-03	-	6.6616e-03	-	α
	128	7.4810e-03		6.6369e-03		
	264	7.4768e-03		6.5526e-03		
	512	7.4747e-03		6.3883e-03		
	1024	7.4652e-03		6.0976e-03		
$\frac{1}{\alpha}$	64	6.3826e-04	-	4.5342e-04	-	1
	128	3.2197e-04	0.9872	2.2819e-04	0.9906	
	264	1.6190e-04	0.9918	1.1461e-04	0.9934	
	512	8.1341e-05	0.9930	5.7549e-05	0.9939	
	1024	4.0768e-05	0.9965	2.8836e-05	0.9969	
$\frac{2}{\alpha}$	64	1.7395e-04	-	1.2293e-04		2
	128	4.5691e-05	1.9287	3.2290e-05	1.9287	
	264	1.1731e-05	1.9616	8.2900e-06	1.9616	
	512	3.0087e-06	1.9631	2.1262e-06	1.9631	
	1024	7.5699e-07	1.9908	5.3495e-07	1.9908	
$\frac{3-\alpha}{\alpha}$	64	3.4871e-04	-	2.4642e-04	-	2
	128	9.3630e-05	1.8970	6.6167e-05	1.8970	
	264	2.4325e-05	1.9445	1.7190e-05	1.9445	
	512	6.2078e-06	1.9703	4.3870e-06	1.9703	
	1024	1.5559e-06	1.9963	1.0996e-06	1.9963	

designed to handle non-smooth solutions, our method outperforms it in terms of both error reduction and the temporal order of convergence. Moreover, in Table 5.5, we provide the spatial convergence orders with respect to both $\mathcal{L}_\infty$ and $\mathcal{L}_2$ norms for fractional orders $\alpha = 0.2, 0.4, 0.6,$ and 0.8.

Here, we have selected the optimal grading parameter $\theta = \frac{2}{\alpha}$ and adapted the time discretization parameter to $N_t = \lceil N_x^{4.5/2} \rceil$, with varying values of N_x. Upon a thorough examination of this table, it becomes clear that the non-polynomial parametric quintic spline scheme employed consistently yields smaller errors and

TABLE 5.2: (Example 5.1) $\mathcal{L}_\infty$ and $\mathcal{L}_2$ errors with temporal order of convergence for $\alpha = 0.9$.

θ	$N_x = N_t$	$\mathcal{L}_\infty$-error	cov.order$_t$	$\mathcal{L}_2$-error	cov.order$_t$	Optimal order
1	64	6.5970e-04	-	4.6922e-04	-	α
	128	3.58106e-04	0.8814	2.5402e-04	0.8853	
	264	1.9326e-04	0.8897	1.3689e-04	0.8919	
	512	1.0396e-04	0.8944	7.3583e-05	0.8955	
	1024	5.5830e-05	0.8970	3.9497e-05	0.8976	
$\frac{1}{\alpha}$	64	4.3935e-04	-	3.1198e-04	-	1
	128	2.2623e-04	0.9575	1.6052e-04	0.9586	
	256	1.1407e-04	0.9877	8.0806e-05	0.9902	
	512	5.7510e-05	0.9881	4.0701e-05	0.9893	
	1024	2.8874e-05	0.9940	2.0426e-05	0.9946	
$\frac{2}{\alpha}$	64	2.2949e-05	-	1.6522e-05	-	2
	128	6.2871e-06	1.8679	4.5036e-06	1.8752	
	264	1.6784e-06	1.9052	1.1977e-06	1.9108	
	512	4.4169e-07	1.9260	3.1427e-07	1.9301	
	1024	1.1422e-07	1.9511	8.1094e-08	1.9543	
$\frac{3-\alpha}{\alpha}$	64	1.9296e-05	-	1.3964e-05	-	2
	128	5.2091e-06	1.8891	3.7519e-06	1.8960	
	264	1.3436e-06	1.9548	9.6425e-07	1.9601	
	512	3.3991e-07	1.9829	2.4323e-07	1.9870	
	1024	8.4934e-08	2.0007	6.0645e-08	2.0038	

achieves a higher spatial convergence order in both the $\mathcal{L}_2$-norm and the $\mathcal{L}_\infty$-norm. In Figure 5.1, we present the $\mathcal{L}_2$-error, achieved for different fractional order values, namely $\alpha = 0.2, 0.4, 0.6$, and 0.8, while comparing the outcomes between a uniform mesh and a graded. It is particularly noteworthy that the error observed on the graded mesh consistently remains lower than that observed on the uniform mesh. Ultimately, we examine the impact of the parameter μ on the actual errors produced by the proposed scheme. Specifically, for the given values $\alpha = 0.8$ and $h = 1/5$, we depict the $\mathcal{L}_2$-error for various μ values within the interval $(0, \tilde{\mu}_0)$, with increments of 0.005, as illustrated in Figure 5.2 for Examples 5.1 and 5.2. It is evident from

TABLE 5.3: (Example 5.1) $\mathcal{L}_\infty$ and $\mathcal{L}_2$ errors with temporal order of convergence with $\theta = \frac{2}{\alpha}$.

α	$N_x = N_t$	$\mathcal{L}_\infty$-error	cov.order$_t$	$\mathcal{L}_2$-error	cov.order$_t$	Optimal order
0.2	64	2.5574e-04	-	1.8059e-04	-	2
	128	7.2837e-05	1.8119	5.1435e-05	1.8119	
	264	1.9918e-05	1.8705	1.4064e-05	1.8707	
	512	5.1064e-06	1.9637	3.6053e-06	1.9638	
	1024	1.2730e-06	2.0040	8.9883e-07	2.0040	
0.4	64	1.0308e-04	-	7.2540e-05	-	2
	128	2.6481e-05	1.9607	1.8641e-05	1.9602	
	264	6.7286e-06	1.9765	4.7360e-06	1.9767	
	512	1.6941e-06	1.9897	1.1923e-06	1.9898	
	1024	4.2457e-07	1.9964	2.9880e-07	1.9965	
0.6	64	6.0417e-05	-	4.2241e-05	-	2
	128	1.5184e-05	1.9924	1.0621e-05	1.9915	
	264	3.6843e-06	2.0430	2.5764e-06	2.0435	
	512	9.2973e-07	1.9865	6.5013e-07	1.9865	
	1024	2.3416e-07	1.9893	1.6375e-07	1.9891	
0.8	64	3.4660e-05	-	2.4741e-05	-	2
	128	9.0477e-06	1.9377	6.4268e-06	1.9447	
	264	2.3287e-06	1.9580	1.6496e-06	1.9620	
	512	5.8917e-07	1.9828	4.1683e-07	1.9846	
	1024	1.4796e-07	1.9935	1.0464e-07	1.9940	

these plots that the choice of μ does exert some influence on the error; however, this influence is marginal. Consequently, in practical applications, any value of μ selected from the interval $(0, \tilde{\mu}_0)$ can be considered suitable.

Example 5.2. *Let's consider the following non-linear TFRDE with variable coefficients*

$$ {}_0^C D_t^\alpha u(x,t) - (2-\sin t)\frac{\partial^2 u(x,t)}{\partial x^2} + (2-\cos t)u(x,t) + u(x,t)^3 = f(x,t), $$

$$ (x,t) \in (0,1) \times (0,1], $$

TABLE 5.4: (Example 5.1) Comparison with method in [91].

		Present method		Method in [91]	
α	$N_t = N_x$	$\mathcal{L}_2$-error	cov.order$_t$	$\mathcal{L}_2$-error	cov.order$_t$
0.3	64	1.0410e-04	-	3.4309e-04	-
	128	2.6801e-05	1.9576	1.1255e-04	1.6080
	256	6.8291e-06	1.9725	3.6549e-05	1.6227
	512	1.7250e-06	1.9851	1.1765e-05	1.6354
	1024	4.3077e-07	2.0016	3.7418e-06	1.6527
0.5	64	7.2937e-05	-	6.4787e-04	-
	128	1.6085e-05	2.1809	2.3765e-04	1.4469
	256	3.7220e-06	2.1115	8.6145e-05	1.4640
	512	9.0824e-07	2.0349	3.1006e-05	1.4742
	1024	2.2803e-07	1.9938	1.1110e-05	1.4807
0.7	64	3.0306e-05	-	1.1575e-03	-
	128	7.7142e-06	1.9740	5.0028e-04	1.2103
	256	1.9395e-06	1.9919	2.1240e-04	1.2360
	512	4.8786e-07	1.9911	8.9080e-05	1.2536
	1024	1.2201e-07	1.9994	3.7040e-05	1.2660

with initial and boundary conditions

$$\begin{cases} u(x,0) = 0, & x \in [0,1], \\ u(0,t) = u(1,t) = 0, & t \in (0,1], \end{cases}$$

where

$$\begin{aligned} f(x,t) = &\left[(1+t) + \left(\frac{t^{\alpha}}{\Gamma(1+\alpha)} + \frac{t^{1+\alpha}}{\Gamma(2+\alpha)}\right)\left((2-\cos t) + 4(2-\sin t)\pi^2 t\right)\right]\sin 2\pi x \\ &+ \left[\left(\frac{t^{\alpha}}{\Gamma(1+\alpha)} + \frac{t^{1+\alpha}}{\Gamma(2+\alpha)}\right)\sin 2\pi x\right]^3. \end{aligned}$$

The exact solution is $u(x,t) = \left(\frac{t^{\alpha}}{\Gamma(1+\alpha)} + \frac{t^{1+\alpha}}{\Gamma(2+\alpha)}\right)\sin 2\pi x.$

TABLE 5.5: (Example 5.1) $\mathcal{L}_\infty$ and $\mathcal{L}_2$ errors with spatial order of convergence for $N_t = \lceil N_x^{4.5/2} \rceil$.

α	N_x	$\mathcal{L}_\infty$-error	cov.order$_x$	$\mathcal{L}_2$-error	cov.order$_x$
0.2	5	6.2489e-04	-	1.4789e-03	-
	10	2.5872e-05	4.5941	5.3986e-05	4.7758
	20	9.8860e-07	4.7099	1.7884e-06	4.9158
0.4	5	1.0569e-03	-	8.2278e-04	-
	10	1.6565e-05	5.9955	1.2069e-05	6.0910
	20	6.3162e-07	4.7130	4.4773e-07	4.7526
0.6	5	3.5292e-04	-	3.0418e-04	-
	10	9.0656e-06	5.2828	6.7494e-06	5.4940
	20	3.5539e-07	4.6729	2.5161e-07	4.7454
0.8	5	2.7238e-04	-	2.4012e-04	-
	10	4.7883e-06	5.8299	3.6263e-06	6.0491
	20	2.1694e-07	4.4641	1.5343e-07	4.5628

The numerical outcomes for Example 5.2 are presented in Tables 5.6, 5.7, and 5.8. Table 5.6 provides a detailed view of the $\mathcal{L}_\infty$ and $\mathcal{L}_2$ errors along with the temporal order of convergence for different fractional orders α, all using the optimal mesh grading $\theta = \frac{2}{\alpha}$. The observations drawn from this table lead to the conclusion that the temporal order of convergence is precisely 2. Additionally, in Table 5.7, we present $\mathcal{L}_\infty$ and $\mathcal{L}_2$ errors along with the spatial order of convergence for various fractional order (α) values (0.2, 0.4, 0.6, 0.8). A careful examination of this table reveals that the errors obtained through our method are significantly lower, demonstrating superior performance, and the convergence order is at least 4.5. Moreover, Table 5.8 provides an insightful comparison between our proposed method and the techniques detailed in [38, 61, 74], offering the $\mathcal{L}_2$-error with spatial order of convergence for $\alpha = 0.3, 0.5, 0.7$ and $N_t = 1000$. The observations from this table undeniably reveal that our method surpassing the spatial order of 2 reported in [61, 74] and 4 reported

TABLE 5.6: (Example 5.2) $\mathcal{L}_\infty$ and $\mathcal{L}_2$ errors with temporal order of convergence with $\theta = \frac{2}{\alpha}$.

α	$N_x = N_t$	$\mathcal{L}_\infty$-error	cov.order$_t$	$\mathcal{L}_2$-error	cov.order$_t$	Optimal order
0.2	64	5.9796e-04	-	4.0924e-04		2
	128	1.4590e-04	2.0350	9.9858e-05	2.0350	
	264	3.5219e-05	2.0505	2.4105e-05	2.0505	
	512	8.4168e-06	2.0650	5.7609e-06	2.0650	
	1024	1.9853e-06	2.0839	1.3588e-06	2.0839	
0.4	64	1.9994e-04	-	1.3780e-04	-	2
	128	5.0313e-05	1.9906	3.4676e-05	1.9906	
	264	1.2623e-05	1.9949	8.6993e-06	1.9949	
	512	3.1611e-06	1.9975	2.1786e-06	1.9975	
	1024	7.9094e-07	1.9988	5.4510e-07	1.9988	
0.6	64	1.6888e-04	-	1.1699e-04	-	2
	128	4.2344e-05	1.9957	2.9334e-05	1.9958	
	264	9.8846e-06	2.0989	6.8476e-06	2.0989	
	512	2.4728e-06	1.9990	1.7130e-06	1.9990	
	1024	6.1840e-07	1.9996	4.2839e-07	1.9996	
0.8	64	1.3700e-04	-	9.5303e-05	-	2
	128	3.4287e-05	1.9984	2.3852e-05	1.9984	
	264	8.2564e-06	2.0541	5.7434e-06	2.0541	
	512	2.0263e-06	2.0267	1.4095e-06	2.0267	
	1024	5.0193e-07	2.0133	3.4916e-07	2.0133	

in [38], thereby positioning itself as the superior choice. Interestingly, the spatial convergence order exceeds the theoretical expectation, as acknowledged in Remark 5.6, and is known to be attainable for specific problem types. Furthermore, it is worth noting that this represents the highest observed spatial convergence order achieved for a non-linear time-fractional reaction-diffusion equation with variable coefficients up to the present date.

TABLE 5.7: (Example 5.2) $\mathcal{L}_\infty$ and $\mathcal{L}_2$ errors with spatial order of convergence for $N_t = \lceil N_x^{4.5/2} \rceil$.

α	N_x	$\mathcal{L}_\infty$-error	cov.order$_x$	$\mathcal{L}_2$-error	cov.order$_x$
0.2	5	1.3292e-02	-	8.7875e-03	-
	10	1.9056e-04	6.1241	1.0689e-04	6.3612
	20	1.6667e-06	6.8371	1.1895e-06	6.4895
0.4	5	1.1892e-02	-	7.8941e-03	-
	10	1.9663e-04	5.9184	1.1044e-04	6.1594
	20	1.7660e-06	6.7988	8.3703e-07	7.0437
0.6	5	1.2640e-02	-	8.3692e-03	-
	10	1.8961e-04	6.0588	1.0871e-04	6.2664
	20	1.7119e-06	6.7912	7.4843e-07	7.1824
0.8	5	1.1979e-02	-	7.9421e-03	-
	10	1.7686e-04	6.0817	1.0267e-04	6.2733
	20	1.6043e-06	6.7845	7.3763e-07	7.1210

TABLE 5.8: (Example 5.2) $\mathcal{L}_2$-error with $N_t = 1000$ and $\theta = \frac{2}{\alpha}$.

α	h	Central [61, 74]	cov.order$_x$	Compact [38]	cov.order$_x$	PQS	cov.order$_x$
0.3	$\frac{1}{5}$	1.5297e-01	-	1.2386e-02	-	9.2174e-03	-
	$\frac{1}{10}$	3.7228e-02	2.0388	7.3879e-04	4.0674	1.2851e-04	6.1643
	$\frac{1}{20}$	9.2426e-03	2.0100	4.4996e-05	4.0372	9.3190e-07	7.1075
0.5	$\frac{1}{5}$	1.4838e-01	-	1.1984e-02	-	8.9277e-03	-
	$\frac{1}{10}$	3.6040e-02	2.0417	7.1490e-04	4.0672	1.2398e-04	6.1700
	$\frac{1}{20}$	8.9431e-03	2.0107	4.3689e-05	4.0323	8.5759e-07	7.1757
0.7	$\frac{1}{5}$	1.4112e-01	-	1.1355e-02	-	8.4724e-03	-
	$\frac{1}{10}$	3.4178e-02	2.0458	6.7739e-04	4.0673	1.1692e-04	6.1790
	$\frac{1}{20}$	8.4754e-03	2.0117	4.1465e-05	4.0300	8.5376e-07	7.0975

5.4 Conclusion

This chapter focused on the development of a highly efficient high-order non-polynomial spline method designed specifically for numerically approximating the non-linear

TFRDE with non-smooth solutions. Our proposed scheme combined the L2-1_σ approximation formula for time discretization with a high-order non-polynomial spline method for spatial derivative handling. Time discretization occurred on a graded mesh, while spatial derivatives were managed on a uniform mesh. Furthermore, in order to solve the resulting non-linear algebraic system, the Newton–Raphson iterative algorithm was chosen as the preferred method due to its quick convergence and straightforward implementation. In addition, the unique solvability of the novel non-polynomial scheme was provided, and its stability was proven via the discrete energy method. The scheme's convergence analysis was also conducted using the discrete energy method, revealing that the method exhibits $\mathcal{O}(N_t^{-\min\{\theta\alpha,2\}}, h^{4.5})$ order of convergence. The spatial convergence order of $\mathcal{O}(h^{4.5})$ had improved upon the performance of the compact finite difference method, with its $\mathcal{O}(h^4)$ order, which had been recognized as the best available outcome at the time. Numerical experiments on two test examples featuring a non-smooth solution, affirmed our scheme's higher-order convergence, validating our theoretical analysis.